Supplementary information

Innovative pH-Buffering Strategies for Enhanced Cycling Stability in Zinc-Iodine Flow Batteries

Phonnapha Tangthuam[a], Suttipong Wannapaiboon[b], Pinit Kidkhunthod[b], Jeng-Lung Chen[c], Chia-Che Chang[c], Chih Wen Pao[c], Phitchapa Ausamanwet Zijdemans[a], Tetsu Yonezawa[d], Manaswee Suttipong[a,*], Soorathep Kheawhom[e,f]

[a]*Department of Chemical Technology, Faculty of Science, Chulalongkorn University, Bangkok 10330, Thailand.*

[b]*Synchrotron Light Research Institute, 111 University Avenue, Muang District, Nakhon Ratchasima 30000, Thailand.*

[c]*National Synchrotron Radiation Research Center, Hsinchu Science Park, Hsinchu 300092, Taiwan.*

[d]*Division of Materials Science and Engineering, Faculty of Engineering, Hokkaido University, Hokkaido, 060-8628, Japan.*

[e]*Department of Chemical Engineering, Faculty of Engineering, Chulalongkorn University, Bangkok 10330, Thailand.*

[f]*Center of Excellence on Advanced Materials for Energy Storage, Chulalongkorn University, Bangkok 10330, Thailand.*

**Corresponding author: Manaswee.S@chula.ac.th*

Flow battery performance

A ZIFB was assembled using a flow battery flex-stak from the Fuel Cell Store. The battery setup included endplate blocks and copper plates, which served as current collectors. Graphite flow field plates were positioned between the copper plates and the electrodes, with silicone rubber gaskets used to form the channel within the flow field plates. Inside the silicone channel, on both the positive and negative sides of the battery, carbon felt (2.5 mm thick) was compressed between the separator and the flow field block. Nafion 115 was employed as the separator.

Electrolytes were circulated through the cell via a dual-channel peristaltic pump (Shenchen Pump, YZ1515x), using Tygon A-60-G tubing (AFL00012). The electrolytes enter at the bottom and exit at the top of the cell. Before conducting electrochemical analysis, the electrolytes were pumped through the cell for at least 30 min to ensure there were no leaks and to fully saturate both the carbon felt electrodes with the electrolytes.

The Nafion 115 membranes were activated by refluxing at 80 °C for 1 hour with 3% hydrogen peroxide and DI water. The membranes were then soaked in 1 M sulfuric acid for 24 h. After activation, the membranes were stored in DI water until further use.

Ionic conductivity

The ionic conductivity of 1M ZnI_2 electrolytes, with and without additives, was measured using EIS. The EIS analysis was conducted over a frequency range of 200 kHz to 0.2 Hz. The ionic conductivity was then calculated, using the following equation:

$$\sigma = \frac{L}{RA}$$

where σ is ionic conductivity (mS/cm), A is the area of the electrode (cm^2), L is the distance between electrode (cm), and R is the intercept-value of the EIS spectral with real impedance axis. The cell configuration for ionic conductivity is shown below:

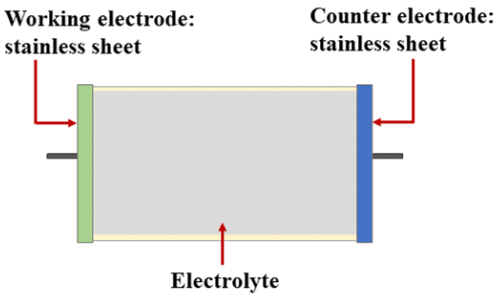

Computation details

Molecular dynamic (MD) simulations were performed, using the GROMACS 2023.2 software package to model the electrolyte solutions, following established protocols [1-3]. The Amber-99 force field was employed to define system parameters [4] while water molecules were represented, using the TIP3P model [5]. Long-range electrostatic interactions were handled, employing the particle-mesh Ewald (PME) method, with a cutoff distance of 1.2 nm and an accuracy threshold of 10^{-5}. Van der Waals forces were also truncated at 1.2 nm. Periodic boundary conditions were applied in all three dimensions (XYZ) to prepare the system.

Before the simulation runs, energy minimization was carried out, using the steepest descent algorithm to eliminate any unfavorable interactions. The systems were initially heated to 500 K over 2 ns, followed by a controlled cooling phase from 500 to 300 K over another 2 ns. To achieve the correct system density, simulations then proceeded for 2 ns under NPT conditions, with a time step of 0.001 ps, using c-rescale barostat to maintain a temperature of 300 K and a pressure of 1 bar. Finally, a 10 ns production run was conducted under NVT conditions, using the Nose-Hoover thermostat to ensure system equilibration at 300 K. The equilibrated system was then used for subsequent data analysis.

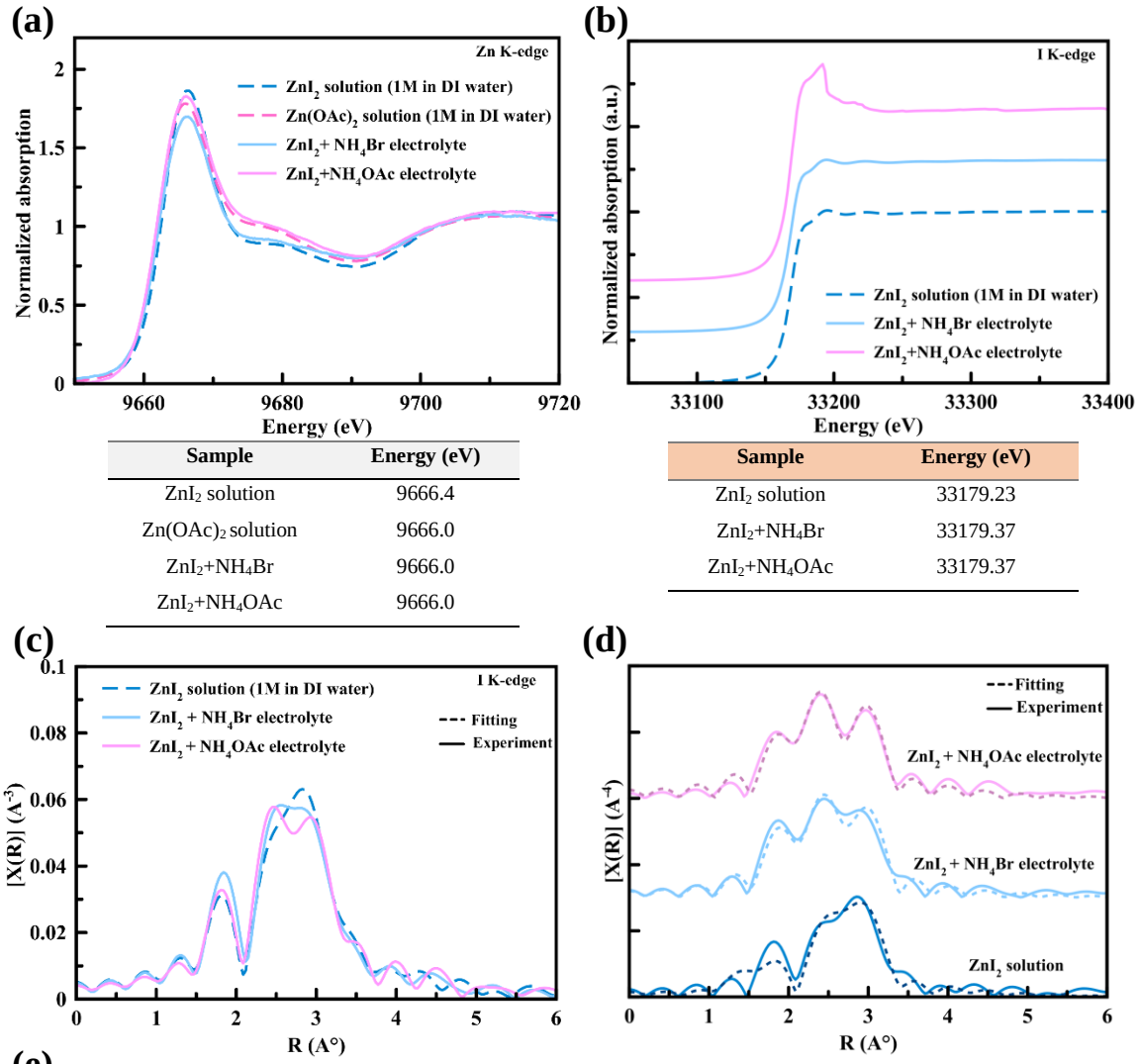

Sample	Energy (eV)
ZnI_2 solution	9666.4
$Zn(OAc)_2$ solution	9666.0
ZnI_2+NH_4Br	9666.0
ZnI_2+NH_4OAc	9666.0

Sample	Energy (eV)
ZnI_2 solution	33179.23
ZnI_2+NH_4Br	33179.37
ZnI_2+NH_4OAc	33179.37

(e)

Sample	CN	R(A°)	$\sigma^2(10^{-3}A^{\circ 2})$	ΔE_0 (eV)	R-factor
		I-Zn			
1M ZnI_2 + 1M NH_4OAc	0.1 ± 0.03	2.7 ± 0.02	1.75 ± 1.91	−44.85 ± 3.42	0.010
1M ZnI_2 solution	6.7 ± 1.6	3.0 ± 0.02	28.48 ± 3.43	−8.51 ± 2.04	0.024
1M ZnI_2 + 1M NH_4Br	0.2 ± 0.1	2.7 ± 0.02	4.47 ± 2.44	−48.07 ± 4.15	0.018
		I-O			
1M ZnI_2 solution	1.9 ± 0.2	2.9 ± 0.02	9.41 ± 2.78	9.00 ± 0.84	0.024
		I-N			
1M ZnI_2 + 1M NH_4OAc	5.4 ± 0.4	3.5 ± 0.01	22.15 ± 1.92	−6.15 ± 0.53	0.010
1M ZnI_2 + 1M NH_4Br	5.1 ± 0.5	3.5 ± 0.01	20.34 ± 2.40	−6.53 ± 0.69	0.018

The list parameters reflect the final best fit. (CN, coordination number; R, interatomic distance; σ^2, Debye-*Waller* factor; ΔE_0, the change of threshold energy; R-factor = $\sum_i(\boldsymbol{data}_i - \boldsymbol{fit}_i)^2/(\boldsymbol{data}_i)^2$; S_0^2 ,the amplitude factor, which was fixed value as a 1.0 from the model compound.)

Figure S1. *(a) Zn K-edge XANES spectra in the standard solution and the electrolytes, (b) Iodine K-edge XANES spectra, (c) EXAFS spectra in 1 M ZnI_2 solution, 1M ZnI_2+1M NH_4Br, and 1M ZnI_2+1M NH_4OAc, (d) Fit results for 1M ZnI_2, 1M ZnI_2+NH_4Br, and 1M ZnI_2+NH_4OAc, and (e) Results for the first shell EXAFS data analysis.*

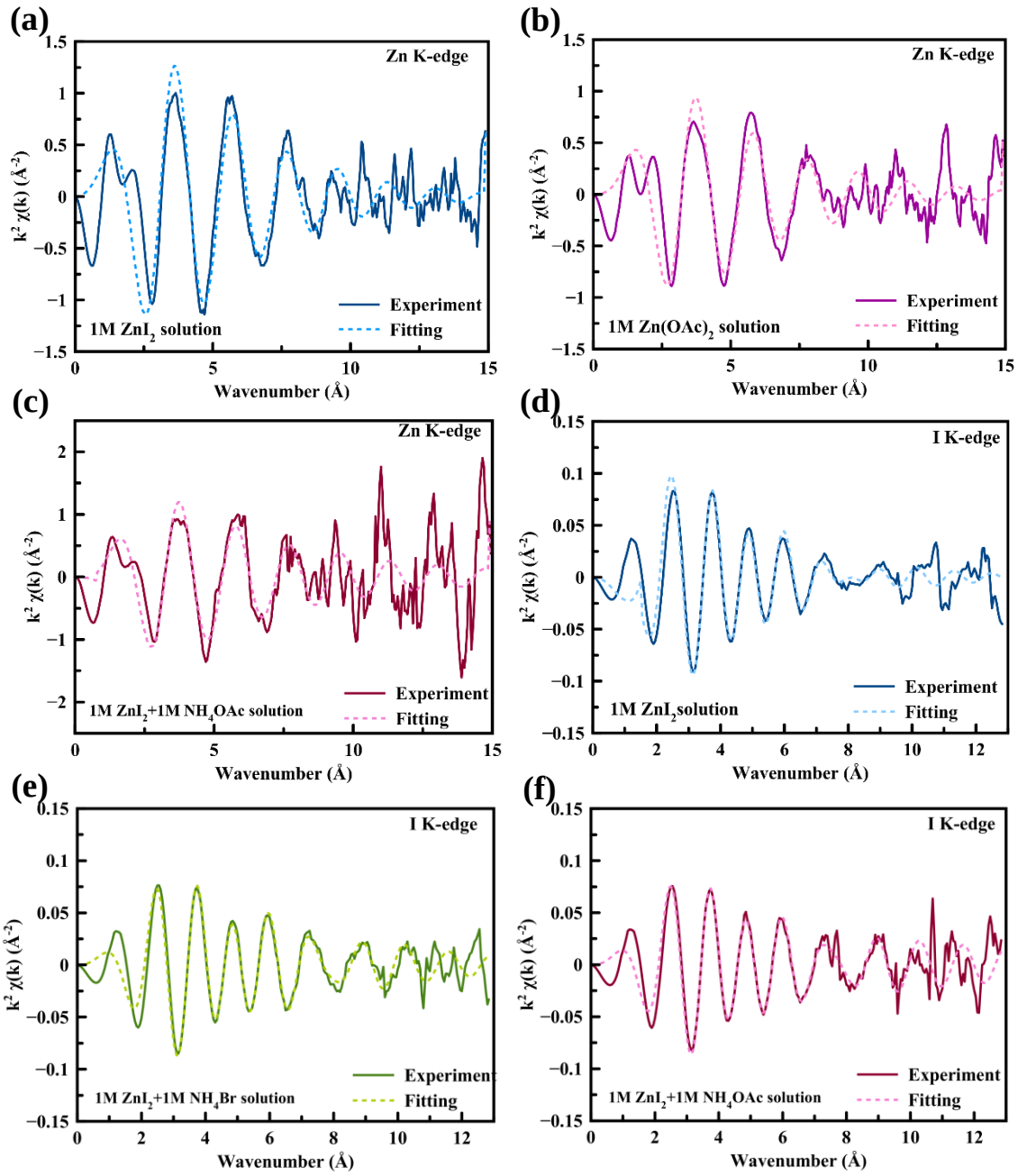

Figure S2. *Zn K-edge EXAFS Fit results for (a) 1M ZnI_2, (b) 1M $Zn(OAc)_2$, and (c) 1M ZnI_2+NH_4OAc solution in k-space. I K-edge EXAFS Fit results for (d) 1M ZnI_2, (e) 1M $Zn(OAc)_2$, and (f) 1M ZnI_2+NH_4OAc solution in k-space.*

Table S1. *EXAFS fitting parameters.*

Scattering Path	Sample	Fitting R-range (Å)
Zn-O	1 M ZnI_2 solution	1.35 - 3.5
	1M $Zn(OAc)_2$ solution	1.35 - 2.9
	1M ZnI_2 + 1M NH_4OAc	1.35 - 3.3
I-O	1 M ZnI_2 solution	3.0 - 10
I-Zn	1 M ZnI_2 solution	3.0 - 10
	1M ZnI_2 + 1M NH_4Br	3.0 - 10
	1M ZnI_2 + 1M NH_4OAc	3.0 - 10
I-N	1M ZnI_2 + 1M NH_4Br	3.0 - 10
	1M ZnI_2 + 1M NH_4OAc	3.0 - 10

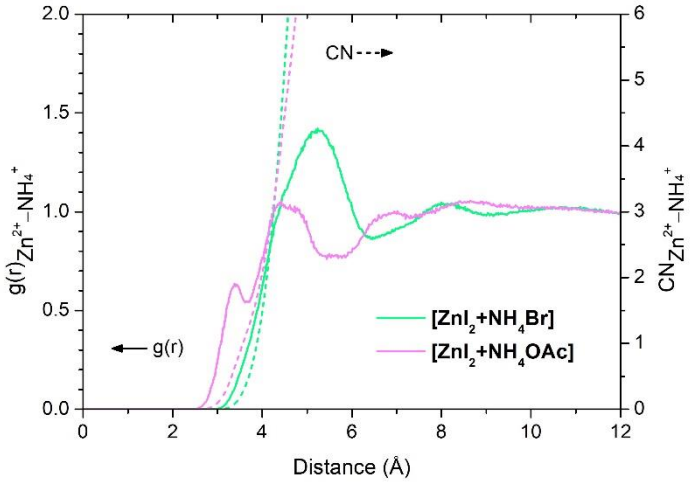

Figure S3. *Radial distribution function (RDF, g(r)) and coordination number (CN) between Zn^{2+} and NH_4^+ in ZnI_2-based electrolytes with the addition of 1 M NH_4Br and 1 M NH_4OAc.*

The RDF peaks at around 4-5 Å and the relatively low CN values indicate that Zn^{2+} does not strongly coordinate with NH_4^+ in either of the electrolyte compositions. The interaction between Zn^{2+} and NH_4^+ is weak and mediated by other ions (such as Br^- or OAc^-) or water rather than direct Zn^{2+}-NH_4^+ bonding.

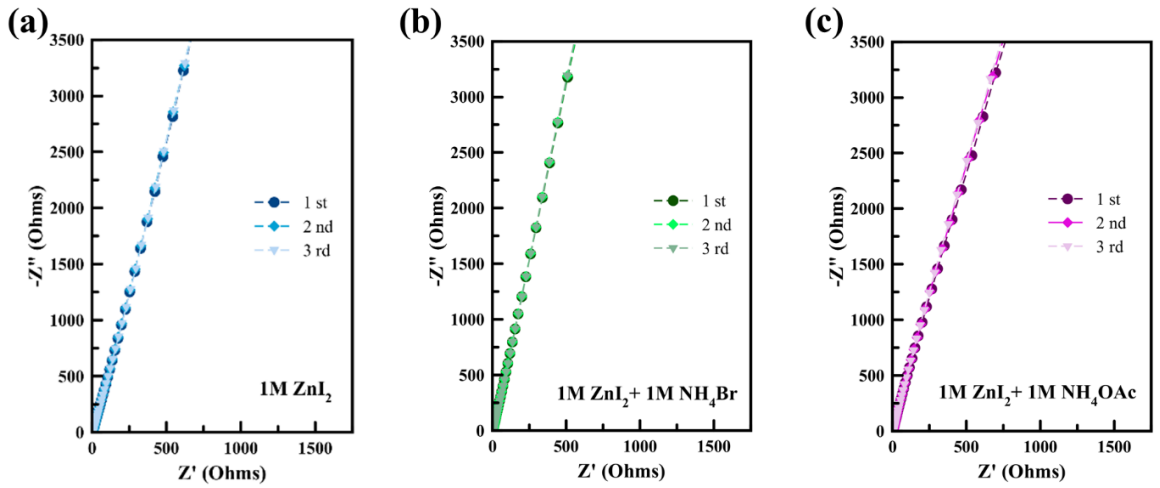

(d)

Ionic conductivity	***1M ZnI_2***	***1M ZnI_2 + 1M NH_4Br***	***1M ZnI_2 + 1M NH_4OAc***
	125.9 mS/cm	*148 mS/cm*	*131.3 mS/cm*

Figure S4. *EIS spectroscopy of (a) ZnI_2, (b) ZnI_2+NH_4Br, and (c) ZnI_2+NH_4OAc electrolyte, and (d) Ionic conductivity results for EIS analysis.*

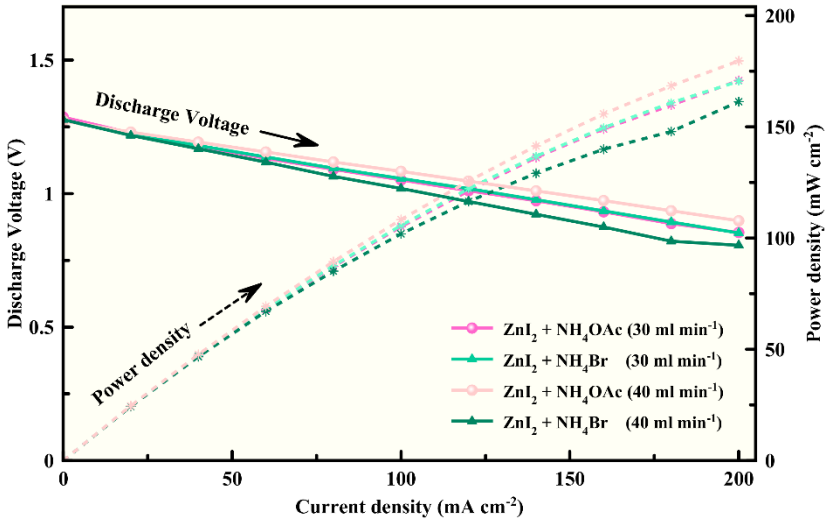

Figure S5. *Discharge voltage and calculated power density for ZIFBs, using different electrolytes at 30 ml min^{-1} and 40 ml min^{-1}.*

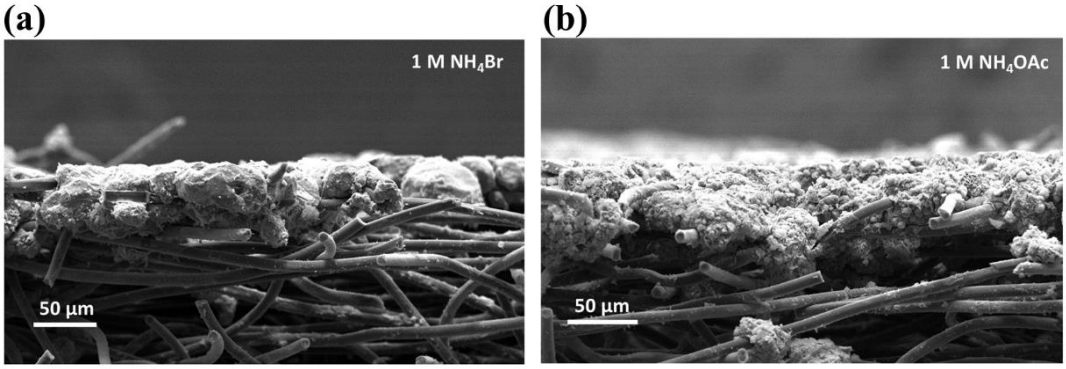

Figure S6. *SEM cross-section morphologies for the electrodeposited layer on carbon fibers at 20 mA cm^{-2} with an aerial capacity of 10 mA h cm^{-2} in (a) 1 M ZnI_2 + 1 M NH_4Br and (b) 1 M ZnI_2 + 1 M NH_4OAc.*

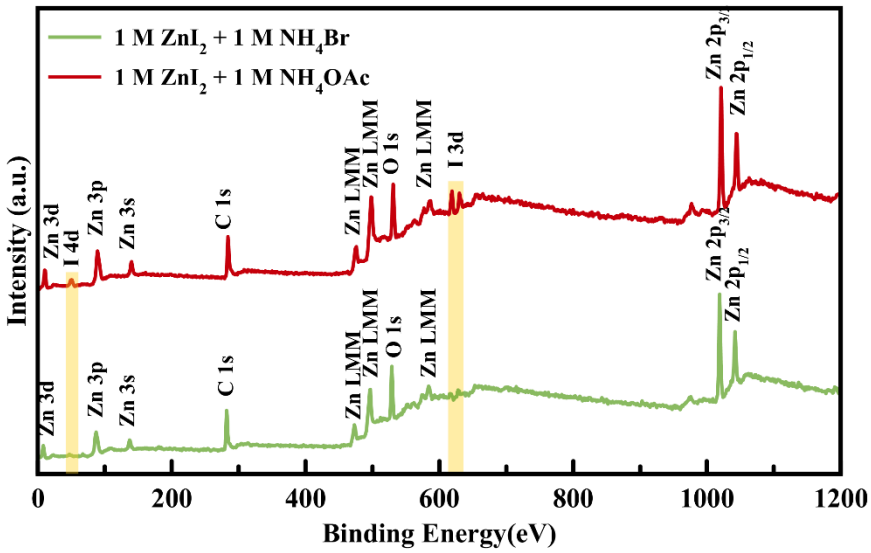

Figure S7. *XPS survey spectra of Zn deposition in different electrolytes.*

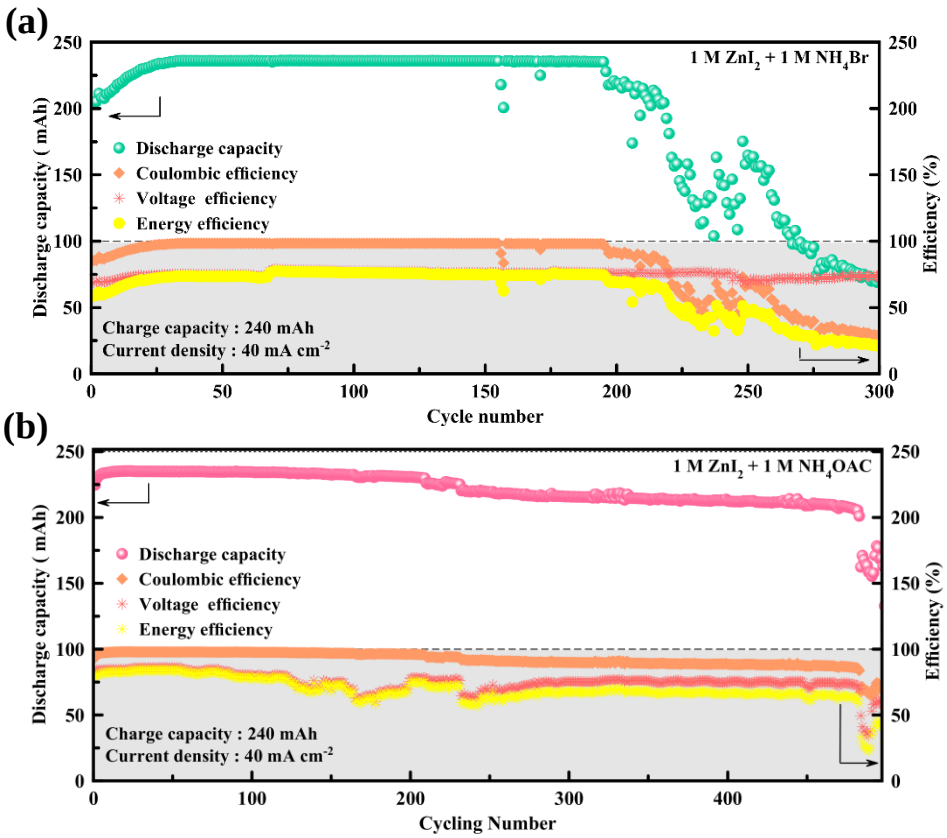

Figure S8. *Discharge capacity and efficiencies of the ZIFBs with (a) NH_4Br, and NH_4OAc at a current density of 40 mA cm^{-2} with charge capacity of 240 mAh.*

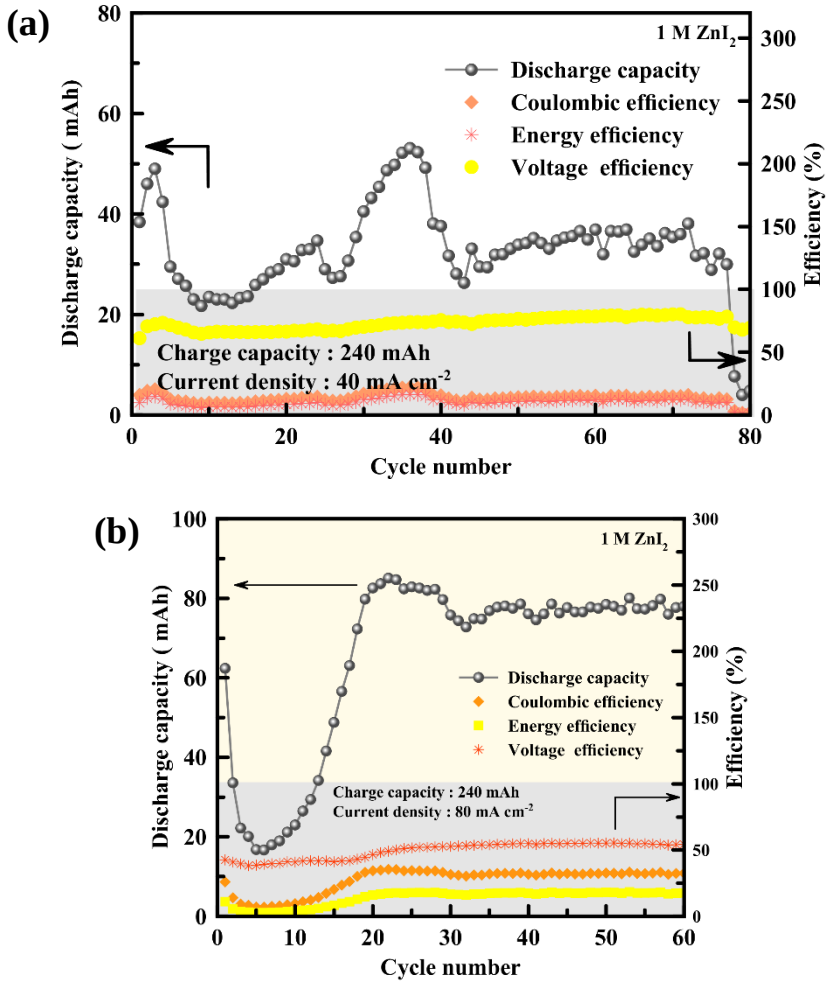

Figure S9. *Discharge capacity and efficiencies of the ZIFBs with 1M ZnI_2 at a current density of (a) 40 mA cm^{-2}, and (b) 80 mA cm^{-2} with a charge capacity of 240 mAh.*

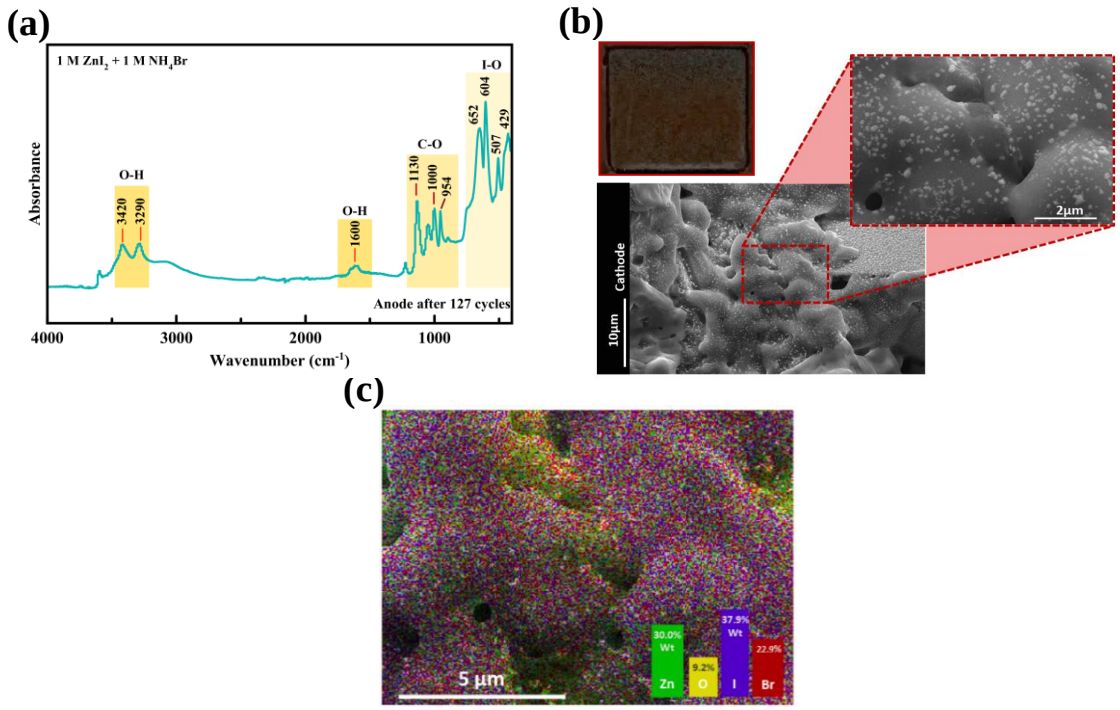

Figure S10. *(a) FTIR spectrum of deposited products on anode after 127 cycles, (b) Optical images, FE-SEM images, and (c) EDS mapping of Zn deposition on cathode after 127 cycles.*

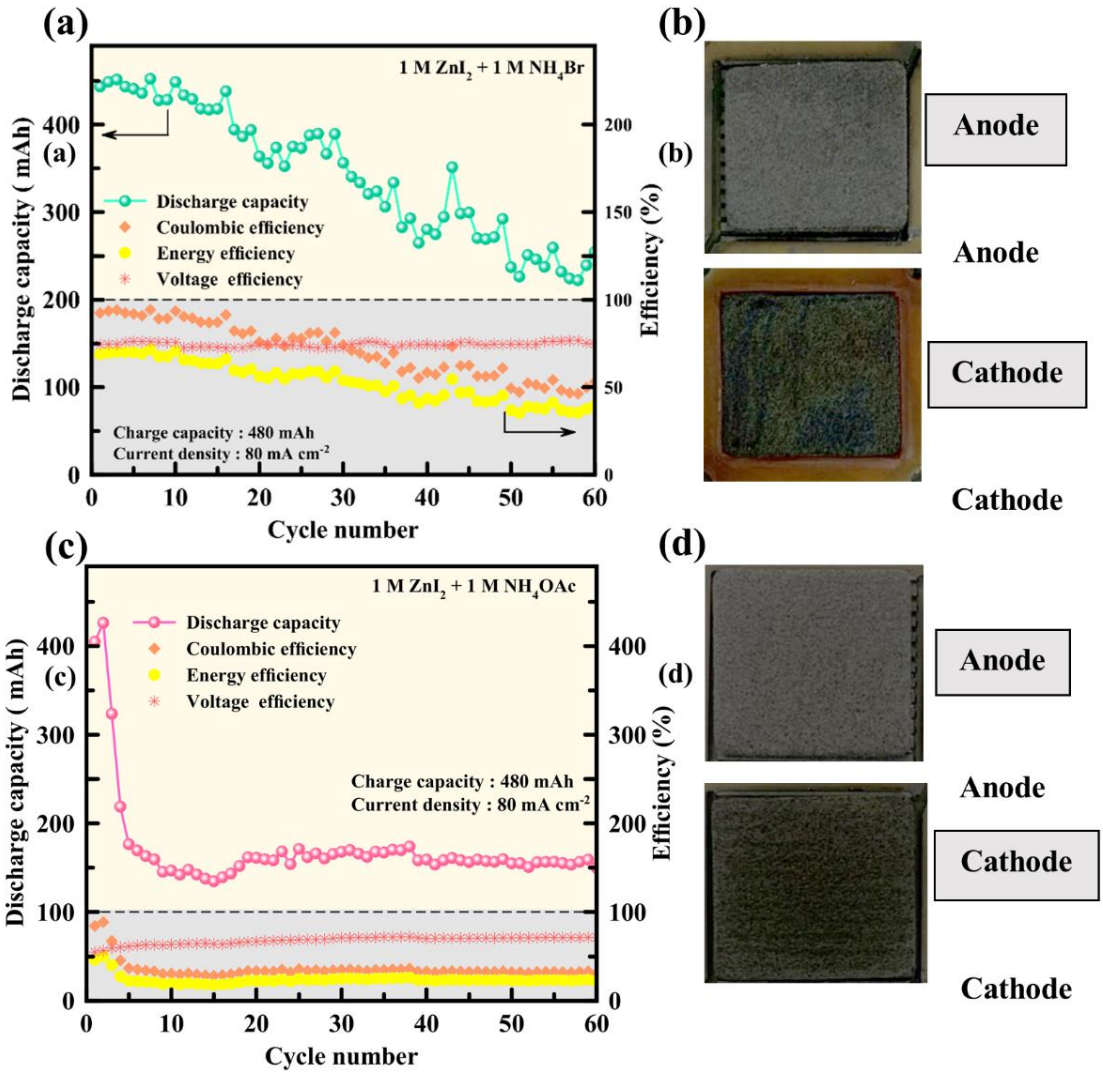

Figure S11. *Discharge capacity and efficiencies of the ZIFBs with (a) NH_4Br and (c) NH_4OAc at a current density of 80 mA cm^{-2} with a charge capacity of 480 mAh, (b) Optical images of post-cycled anode and cathode with (b) 1 M ZnI_2 + 1 M NH_4Br and (d) 1 M ZnI_2 + 1 M NH_4OAc, under a current density of 80 mA cm^{-2} with charge capacity 480 mAh.*

References

1. D. Van Der Spoel, E. Lindahl, B. Hess, G. Groenhof, A. E. Mark and H. J. C. Berendsen, *J. Comput. Chem.*, 2005, **26**, 1701-1718, DOI: 10.1002/jcc.20291.
2. M. J. Abraham, T. Murtola, R. Schulz, S. Páll, J. C. Smith, B. Hess and E. Lindahl, *SoftwareX*, 2015, **1-2**, 19-25, DOI: 10.1016/j.softx.2015.06.001.
3. A. A. Mark Abraham, Cathrine Bergh, Christian Blau, Eliane Briand, Mahesh Doijade, and etc., *GROMACS 2023.2 Source code*, Zenodo, 2023.
4. J. Wang, R. M. Wolf, J. W. Caldwell, P. A. Kollman and D. A. Case, *J. Comput. Chem.*, 2004, **25**, 1157-1174, DOI: 10.1002/jcc.20035.
5. W. L. Jorgensen, J. Chandrasekhar, J. D. Madura, R. W. Impey and M. L. Klein, *J. Chem. Phys.*, 1983, **79**, 926-935, DOI: 10.1063/1.445869.